Interaction of Alkene Radical Cations with Solvent Molecules As Described with Density Functional Theory

M. Mohr and H. Zipse*

Institut fur Organische Chemie, TU Berlin, Strasse d. 17. Juni 135, D-10623 Berlin, Germany

D. Marx and M. Parrinello

Max-Planck-Institut für Festkörperforschung, Heisenbergstrasse 1, D-70569 Stuttgart, Germany

Received: July 17, 1997[⊗]

Structures and energetics of several distonic radical cations, in particular the adducts between ethylene radical cation and water, ammonia, and hydrogen fluoride, are investigated using various density functional and post Hartree−Fock methods. Both the structure and the energetics of the $[CH_2CH_2{\cdot}NH_3]^{\bullet+}$ and $[CH_2CH_2{\cdot}HF]^{\bullet+}$ adducts with pronounced covalent and electrostatic bonding, respectively, are well described using the gradient-corrected BLYP functional. The intermediate bonding situation of $[CH_2CH_2{\cdot}OH_2]^{\bullet+}$, in particular the structure, is not well described with BLYP, whereas the binding energy is in surprisingly close agreement with post Hartree−Fock methods. The reason for this behavior is analyzed in terms of the different contributions to the total energy, and it is shown that the deficiency is remedied when the nonlocal hybrid functional BHLYP is used. Finally, it is found that the performance of BLYP improves on inclusion of additional water molecules. Thus the weakness of BLYP to describe the structure of the $[CH_2CH_2{\cdot}OH_2]^{\bullet+}$ radical cation is a specific exception rather than typical for the large class of distonic radical cations. One can therefore expect BLYP to provide a realistic description of alkene radical cations in aqueous solution.

Introduction

The chemistry of alkene radical cations has received increasing attention recently due to the possible involvement of these reactive intermediates in alkene oxidation reactions. Most of the reactions are carried out in polar solvents such as acetonitrile, water, dichloromethane, and alcohols or mixtures thereof. A detailed theoretical study must therefore consider the interaction of radical cations with the solvent in an explicit manner. Two borderline cases may be expected in this context. The first case might best be described as "unreactive solvation", in which the solute−solvent interaction does not lead to the formation of covalent bonds (Scheme 1, **A**). This type of solvation can in principle be described with simple empirical potentials, even though the presence of charged substrates might make it necessary to employ polarizable models.[1] The second case can be termed "reactive solvation", in which a covalent bond is formed between solvent and solute (Scheme 1, **B**). The center of positive charge in this adduct is separated from the center of unpaired spin density through a methylene group. According to Radom et al., such species are termed β-distonic radical cations.[2] A recent investigation of the interaction between single water molecules and ethylene radical cation (**1**) revealed the formation of distonic radical cation **5a** without barrier in the gas phase (Figure 1).[3] The strength of the C−O bond formed in this process is, however, rather weak, and the structure of distonic ion **5a** changes markedly on inclusion of additional water molecules. It thus appears that a final decision between reactive and unreactive solvation for ethylene radical cations can only be expected from a full quantum mechanical solution simulation. One theoretical approach, which has recently been used to obtain a detailed picture of the structure of water,[4] the hydration of simple ions,[5] and simple reactions in water,[6] is the Car−Parrinello molecular dynamics method (CPMD).[7] This method employs density functional theory together with coupled dynamics of the ionic and electronic system to achieve ab initio dynamics in an economic fashion. To investigate whether density functional theory is suitable to study radical cations in solution, we study here the interaction of the ethylene radical cation as a model for alkene radical cations with water and other small nucleophiles.

SCHEME 1: Schematic Representation of Unreactive (A) and Reactive (B) Solvation

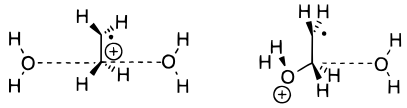

A **B**

Theoretical Methods

Over the last decade approximate density functional theory (DFT) methods developed into a promising tool for the description of open shell systems. Unfortunately, bond dissociation energies tend to be overestimated, which has been traced back to an inadequate treatment of exchange terms.[8] When the gradient of the electron density is included, as for example in the semilocal Becke−Lee−Yang−Parr functional (BLYP),[9] the DFT-typical overbinding is reduced and the results are found to be in good agreement with experimental and high-level ab initio results. The performance of gradient-corrected density functionals for first-, second-, and third-row homonuclear diatomics is superior to second-order Møller−Plesset perturbation theory (MP2) and even configuration interaction (Cl) methods,[10] especially for the group II dimers, which are known to be badly described by conventional Hartree−Fock (HF) and MP*x* schemes. There are also some open shell species known in which DFT methods are superior to much more elaborate ab initio methods like QCISD(T) or MP4.[11]

A successful approach to improve the DFT treatment of exchange energy contributions was initiated by Becke.[12] The

[⊗] Abstract published in *Advance ACS Abstracts,* October 15, 1997.

S1089-5639(97)02344-X CCC: $14.00

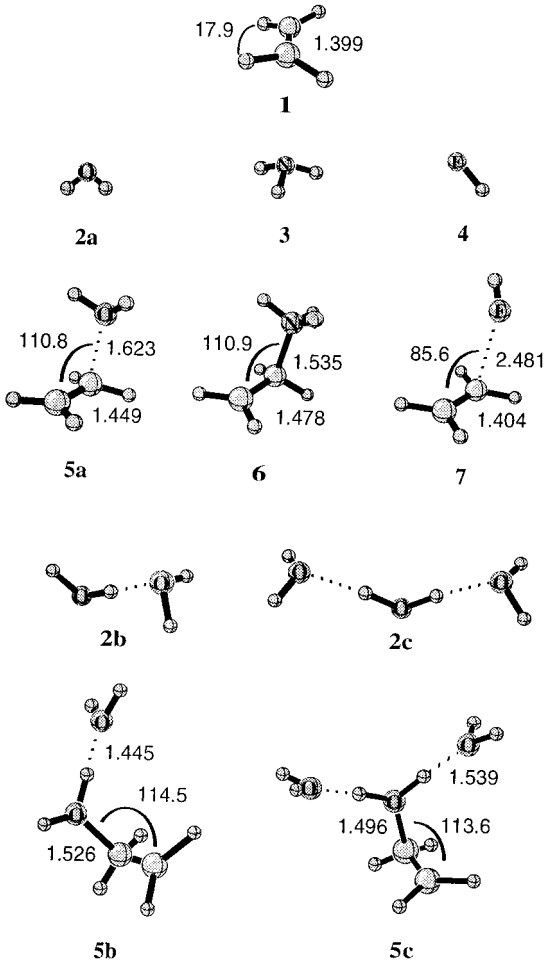

Figure 1. BHLYP/6-31+G(d,p) optimized geometries of the structures **1**−**7**.

basic idea is to mix in HF exchange in the sense of evaluating the exchange energy of the Slater determinant using Kohn−Sham orbitals. Various such nonlocal schemes now exist. In particular, we employed the "half-and-half" BHLYP and the three parameter fitted B3LYP functional as implemented in Gaussian 94.[13]

Most of the calculations were performed using the Gaussian94 Rev. B.3 suite of programs. The structures were fully optimized at the indicated level of theory, with standard basis sets as implemented in the program. MP2 and all density functional stationary points were characterized by calculation of the harmonic frequencies using analytical second derivatives of the energy with respect to the Cartesian coordinates. The CCSD force constants were determined by numerical differentiation. Reference determinants constructed from Kohn−Sham orbitals are known to be less spin contaminated than those calculated with perturbation theory schemes.[14] The largest expectation value of $\langle s^2 \rangle$ for doublet DFT reference determinants was 0.754 and 0.762 for MP2, so the frequent problems[15] caused by spin contamination of UMP*x* wave functions did not surface in this study. In all DFT calculations the SCF convergence criterion was set to 10^{-8} au, and for each atom the standard (75 302) grid was used for the numerical integration procedure. To facilitate the comparison of results obtained at various levels of theory, no corrections of zero-point energies have been included.

In addition to the calculations using Gaussian basis sets we also performed stationary point calculations with a plane wave (PW) basis set and effective core potentials in conjunction with the BLYP functional using the CPMD code.[16] In particular, we represented the heavy atom 1s electrons by norm-conserving pseudopotentials of the Troullier−Martins type[17] and expanded the valence orbitals in a set of plane waves with a kinetic energy cutoff of 70 Ry in a cubic box with edge length of 20 au; we did not impose periodic boundary conditions in these calculations. Note that the use of plane wave basis sets avoids the occurrence of basis set superposition errors (BSSE).

Results and Discussion

Energetics. To find the minimal basis set necessary for the proper description of the binding energy in distonic ion **5a**, we employed the BLYP and MP2 method together with a variety of different basis sets (Table 1). Density functional calculations are known to be much less basis set dependent than conventional perturbation theory. Inspection of the bond dissociation energies (BDEs) summarized in Table 1 shows that the inclusion of a heavy atom diffuse basis function lowers the binding energy by 7−9 kcal/mol even for otherwise reasonably large basis sets. Even when the heavy atom core electrons are kept frozen, as in the CEP effective core potential,[18] the large basis set limit is reproduced with reasonable accuracy. Increasing the flexibility of the basis to a triple-ζ contraction as well as including polarization functions with higher angular momenta than l+1 does apparently not lead to further improvement of the binding energy. The BSSE was calculated according to the counterpoise

TABLE 1: Summary of Structural Data and Energetics for 1 and 5a Calculated at the BLYP and MP2 Level of Theory in Combination with Several Basis Sets

	structure **1**		structure **5a**			
basis set	*d*(CC) [Å]	*t*(HCCH) [deg]	*d*(CC) [Å]	*d*(CO) [A]	*a*(CCO) [deg]	BDE [kcal/mol]
BLYP						
CEP-31+G(d)[a]	1.435	26.9	1.453	1.929	108.2	25.5
6-31G(d)	1.402	30.5	1.428	1.924	108.4	33.4
6-31G(d,p)	1.399	31.5	1.426	1.944	107.7	32.9
6-31+G(d,p)[b]	1.399	31.9	1.421	2.033	106.7	25.7
6-311G(d)	1.392	32.5	1.424	2.050	106.0	34.6
6-311+G(d,p)	1.392	32.9	1.414	2.075	105.7	25.3
6-311++G(3df,2p)	1.387	35.8	1.411	2.050	106.0	24.6
PW[c]	1.377	35.8	1.399	2.043	104.5	23.7
MP2						
6-31G(d)	1.417	5.0	1.458	1.613	111.1	31.9
6-31G(d,p)	1.415	5.0	1.457	1.609	111.1	31.4
6-31+G(d,p)	1.415	7.8	1.456	1.618	111.3	25.9
6-311G(d)	1.418	5.1	1.463	1.586	111.5	34.5

[a] Effective core potential according to ref 18. [b] The BSSE for this basis set amounts to 1.2 kcal/mol. [c] Plane wave basis set. See Theoretical Methods section for details.

TABLE 2: Summary of Structural Data and Energetics for 1 and 5a Calculated with Different Density Functionals and at the QCISD Level of Theory

	structure **1**		structure **5a**			
method	*d*(CC) [Å]	*t*(HCCH) [deg]	*d*(CC) [Å]	*d*(CO) [Å]	*a*(CCO) [deg]	BDE [kcal/mol]
6-31+G(d,p)						
HF	1.403	0.1	1.465	1.596	110.4	10.3
SVWN	1.366	37.4	1.440	1.612	111.4	40.5
SLYP	1.362	38.6	1.444	1.585	111.2	45.4
BVWN	1.404	29.1	1.414	2.168	104.7	22.4
BP86	1.395	32.6	1.437	1.816	109.8	28.4
BLYP	1.399	31.9	1.421	2.033	106.7	25.7
B3LYP	1.397	27.6	1.433	1.794	109.6	25.0
BHLYP	1.399	17.9	1.448	1.623	110.1	24.4
MP2	1.415	7.8	1.456	1.618	111.3	25.9
QCISD	1.412	15.6	1.411	1.636	110.1	24.4
CCSD	1.414	12.2	1.449	1.608	110.3	23.3
QCISD						
6-311++G(2d,p)	1.408	18.4	1.461	1.619	111.1	24.8
6-311++G(2df,p)	1.403	18.9	1.458	1.604	111.0	25.7

method and amounts to 1.2 kcal/mol at the BLYP/6-31+G(d,p) level of theory. Because plane wave basis functions are not assigned to any atomic center, binding energies exhibit no BSSE. The BLYP/PW value calculated here is virtually identical to the largest Gaussian basis set used, i.e. BLYP/6-311++G(3df,2p) binding energy, if the BSSE of about 1.2 kcal/mol is taken into account.

When the MP2 Hamiltonian is used, the same basis set effect is found. Inclusion of heavy atom diffuse basis functions weakens the bond by 5.5 kcal/mol. Using more elaborate theoretical approaches like the QCISD or CCSD scheme with the 6-31+G(d,p) basis set does not lead to any significant improvement of the binding energy, even with significantly larger basis sets (Table 2). The binding energy amounts to 25.7 kcal/mol at the QCISD/6-311++G(2df,p) level of theory. As expected, the local density approximation, here SVWN, leads to tremendous overbinding of the magnitude of the binding energy itself, which is significantly decreased by Becke's semilocal exchange correction (B88). Hartree−Fock theory shows the opposite effect and is therefore also eliminated from the list of useful methods for the present purpose. The good agreement of the BVWN binding energy with the CCSD value is caused by mutual compensation of errors. The gradient correction on the exchange energy is larger than the correlation energy gradient correction. Usually these corrections have opposite signs. Therefore the remainder of the exchange error which is not compensated by the B88 semilocal correction is compensated by the error due to the use of a local correlation functional. Using a functional that is only gradient corrected for the correlation term (SLYP), the overbinding is even increased for the same reason mentioned above.

Structure. The survey of structural data given in Table 1 shows two major points of discrepancy between the MP2 and BLYP results. First, the twisting of the ethylene radical cation **1** is enlarged to an average value of 32° in the BLYP calculations compared to an average angle of 6° for different basis sets for the MP2 Hamiltonian. In a valence-bond picture this twisting originates from an interaction of the $^2B_{2u}$ and the $^2B_{2g}$ states of planar geometry. Breaking the symmetry from D_{2h} to D_2 results in a nonzero mixing term $\langle ^2B_{2u}|^{12}B_{2g}\rangle$.[19] From a molecular orbital point of view this can be understood as a compromise between common π-bonding, which is optimal in planar geometry, and hyperconjugation, which prefers the perpendicular structure. Indeed there is experimental evidence for a twisting of ethylene radical cations. From vacuum ultraviolet studies of a series of Rydberg states of ethylene a twisting angle of 25° was concluded.[20] These findings are supported by an analysis of the vibrational structure of photoelectron spectra of ethylene and in line with early high-level ab initio CI calculations[22] which predict a 23° twisting angle. Our own high-level QCISD/6-311++G(2df,p) calculations predict 19° (Table 2). Thus, the MP2 and BLYP results can be understood as the limiting cases of the real bonding situation. MP2 underestimates the contributions from the $^2B_{2g}$ state, whereas BLYP overestimates the excited-state contribution. This effect can be attributed to the already mentioned deficiency in the correct description of exchange terms. Gradual inclusion of HF exchange contribution within DFT in the series BLYP, B3LYP, and BHLYP leads to an almost steady transition from a twisting angle of 33° obtained with semilocal functionals to the low MP2 value of 8°.

Second, comparison of the BLYP and MP2 geometries of ion **5a** in Table 1 shows a major difference in the C−O bond lengths. For the BLYP functional the carbon−oxygen bond length is larger by 0.415 Å despite the fact that BLYP and MP2 energetics are basically identical. To understand the origin of this surprisingly large difference, we optimized the structure of **5a** with several other conventional and DFT ab initio methods (Table 2). The first remarkable point is the geometry calculated with the exchange functional of Slater in combination with the correlation functional of Vosko, Wilk, and Nusair (VWN).[23] This functional yields results comparable to the MP2 values for the C−C and C−O bond length as well as the C−C−O bond angle, although this functional is completely local and therefore the least sophisticated functional used in this study. Adding Becke's semilocal exchange correction to Slater's exchange functional (BVWN) yields the largest C−O bond length (2.168 Å) among the density functional methods. Nevertheless, the SLYP functional gives the shortest carbon−oxygen bond among the methods used here. Using the gradient-corrected correlation functional of Perdew[24] (P86) instead of the LYP functional yields a shorter carbon−oxygen bond of 1.816 Å and a 2.7 kcal/mol increase in binding energy. There are obviously two effects influencing the structural and energetic properties of distonic ion **5a** in semilocal DFT calculations. The first one is caused by the B88 gradient correction term. If this contribution is included, the long-bonded distonic ion **5a** is found and at the same time the dramatic overbinding of the SVWN functional is reduced to 22.4 kcal/mol. This effect is observed for the local VWN correlation functional as well as the nonlocal LYP functional. The second much less dramatic effect influencing the geometry is due to the correlation functional, as shown by replacement of the LYP correlation functional by P86.

The hybrid functionals B3LYP and BHLYP behave somewhat differently. Again, as found for the twisting of ethylene radical

TABLE 3: Summary of Selected Structural Data and Energetics for Distonic Ions 5a-c, 6, and 7[a]

	BLYP	B3LYP	BHLYP	QCISD	MP2
structure **6**					
d(CN) [Å]	1.596	1.561	1.534	1.541	
θ(CCHH) [deg][b]	128.2	127.0	126.3	126.5	
BDE [kcal/mol]	52.0	56.8	58.3	59.8	
structure **5a**					
d(CO) [Å]	2.033	1.794	1.623	1.636	1.618
θ(CCHH) [deg]	158.2	146.4	137.7	137.6	137.2
BDE [kcal/mol]	25.7	25.0	24.4	24.4	25.9
structure **7**					
d(CF) [Å]	2.316	2.392	2.481	2.522	
θ(CCHH) [deg]	173.8	176.9	179.5	178.6	
BDE [kcal/mol]	10.0	10.3	11.2	12.6	
structure **5b**					
d(CO) [Å]	1.657		1.526		1.541
θ(CCHH) [deg]	136.7		130.9		131.4
BDE [kcal/mol][c]	42.9		44.7		46.6
Structure **5c**					
d(CO) [Å]	1.584		1.496		1.513
θ(CCHH) [deg]	131.9		128.3		129.2
BDE [kcal/mol][c]	58.4		61.7		64.0

[a] All calculations with the 6-31+G(d,p) basis set. [b] As defined in Scheme 2. [c] For the dissociation into **1** and **2b**, and **2c** respectively.

cation, gradual inclusion of HF exchange leads to a steady transition between the borderline cases of the semilocal functional BLYP and the high-level ab initio method QCISD. For the B3LYP functional a bond length of 1.794 Å is found; for the BHLYP functional the bond length is 1.623 Å, which is, as for the ethylene radical cation, comparable to the QCISD values. Surprisingly, the binding energy changes by only 1.3 kcal/mol when HF exchange is included, despite the dramatic change in C−O bond length. That the bonding situation in **5a** is difficult to describe even for highly correlated methods can be taken from the QCISD/6-31+G(d,p) and CCSD/6-31+G(d,p) results. Even though a short bond is predicted in both cases, the crucial C−O bond distance varies quite significantly (1.636 Å for QCISD vs 1.608 Å for CCSD), although these two methods are expected to yield very similar results.

We therefore recalculated the equilibrium structure of **5a** at the QCISD/6-311++G(2d,p) and QCISD/6-311++G(2df,p) level of theory. The extension of the basis set for the CCSD method proved prohibitively expensive. The problem here is the lack of analytical gradients, which makes such an optimization extremely costly. The results for the QCISD/6311++G-(2d,p) and QCISD/6-311++G(2df,p) calculations are given in Table 2. A steady transition to shorter C−O bond length is found as the flexibility of the basis set is increased. For the most flexible 6-311++G(2df,p) basis set the C−O bond distance is 1.604 Å, very close to the CCSD/6-31+G(d,p) value of 1.608. We therefore take the QCISD/6-311++G(2df,p) structure as the reference for the evaluation of the DFT results.

Related Systems. To understand whether these trends are systematically inherent in DFT methods or whether we found a unique pathology concerned with distonic ion **5a**, we also looked at the distonic ions obtained by the addition of ammonia (**3**) or hydrogen fluoride (**4**) to ethylene radical cation **1**. Ammonia and hydrogen fluoride are expected to form stronger and weaker bonds with the ethylene radical cation, respectively, and thus to alter significantly the bonding situation relative to the water adduct **5a**.

Distonic ion **6** is formed through the addition of ammonia to ethylene radical cation (Figure 1). A similar but much less pronounced trend as for **5a** is found for ion **6** (Table 3). The carbon−nitrogen bond length decreases by 0.055 Å if QCISD instead of BLYP is used. As observed for ion **5a**, there is a steady transition from semilocal DFT results to the QCISD values by the gradual inclusion of nonlocal HF exchange to the density functional for the energetics as well as for structural parameters. In contrast to distonic ion **5a**, the binding energy in distonic ion **6** increases by 7.8 kcal/mol on going from the BLYP to the QCISD level of theory. The trend is slightly different for distonic ion **7**, which is formed by the reaction of hydrogen fluoride with ethylene radical cation (Figure 1). The QCISD calculation yields a bond length of 2.522 Å, compared to a BLYP value of 2.316 Å, and the QCISD binding energy for that ion amounts to 12.6 kcal/mol.

SCHEME 2: Definition of the Angle *θ*(CCHH) Describing the Degree of Pyramidalization at C_1 in Adduct 5a

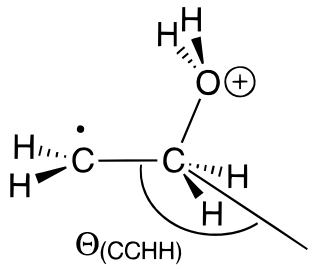

If the degree of pyramidalization at C_1, as defined in Scheme 2, is taken as an indicator of covalent bond formation between the reaction partners, one must conclude that the bonding situation in distonic ion **6** is entirely different from that in distonic ion **7**. Distonic ion **6** shows significant pyramidalization at C_1 with a CCHH dihedral angle of 126.3° for the BHLYP functional. The ethylene radical cation moiety of distonic ion **7**, in contrast, shows the planar geometry (179.5°) also found for the free ethylene radical cation **1** (180.0°). These findings are in line with the observed binding energies of these species. The binding energy of ion **6** calculated at the BHLYP/6-31+G-(d,p) level of theory amounts to 58.3 kcal/mol, whereas system **7** yields a much smaller binding energy of 11.2 kcal/mol.

We can conclude at this point that the observed differences in bond lengths are not a common feature of the description of distonic ions by density functional methods. Distonic ion **5a** can best be understood as an intermediate case between covalent binding and a more electrostatic interaction and therefore might be difficult to handle with some DFT methods. The binding in distonic ion **7** arises predominantly from ion−dipole-type electrostatic interactions, whereas ion **6** shows an almost fully established covalent C−N single bond. This conclusion is also supported by the degree of pyramidalization as well as the C−N bond length of 1.541 Å (compared to 1.47 Å for methylamine CH_3NH_2).

Analysis. To shed some light on the origin of these effects, the binding energy was decomposed into the components of the Kohn−Sham energy in the following way:

$$E_{KS} = E_{Nuc} + E_{le} + E_{Coul} + E_X + E_C \quad (1)$$

$$\Delta E_{KS} = \Delta\Sigma + \Delta E_X + \Delta E_C \quad (2)$$

$$\Delta E_X = {}^1/_2\Delta E_{XB88} + {}^1/_2\Delta E_{XHF} \quad (3)$$

In general, the Kohn−Sham energy E_{KS} can be subdivided into classical nuclear repulsion energy, one-electron energy, which consists of the kinetic and the potential energy of the electrons, the Coulomb repulsion of the electrons, and exchange and correlation energies. The nuclear repulsion energy, the one-electron contribution, and the electronic Coulomb repulsion are not discussed individually, because these quantities do not

TABLE 4: Components of the Binding Energy for the Reaction Pathway for Addition of Water to Ethylene Radical Cation and the Equilibrium Geometries of Distonic Ions 5a, 6, and 7[a]

	structure **1** r(CX)[c]								
	2.1 Å	2.0 Å	1.9 Å	1.8 Å	1.7 Å	1.6 Å	structure **5a**	structure **6**	structure **7**
					BLYP/6-31+G(d,p)				
$\Delta\Sigma$[b]	13.1	8.7	3.4	−3.1	−11.3	−22.5	10.5	−4.1	3.9
ΔE_x	6.0	9.8	14.2	19.5	26.1	34.7	8.3	47.1	2.9
ΔE_c	6.5	7.2	7.8	8.5	9.2	10.1	6.9	9.0	3.2
ΔE_{Tot}	25.6	25.7	25.4	24.9	24.0	22.3	25.7	52.0	10.0
					BHLYP/6-31+G(d,p)				
$\Delta\Sigma$[b]	12.6	10.2	6.5	2.7	−4.3	−14.6	−11.9	−5.1	2.7
$\Delta^1/_2E_{XB88}$	2.4	3.4	4.9	6.8	9.5	13.6	12.5	23.8	2.2
$\Delta^1/_2E_{XHF}$	0.3	1.5	3.6	5.4	9.5	15.1	13.7	27.7	3.4
ΔE_x	2.7	4.9	8.5	12.2	19.0	28.7	26.2	51.5	5.6
ΔE_c	6.6	7.3	8.0	8.6	9.4	10.2	10.0	11.9	2.9
ΔE_{Tot}	21.9	22.4	23.0	23.5	24.1	24.3	24.4	58.3	11.2

[a] All values given in kcal/mol. [b] Denotes the sum of the differences in nuclear repulsion, one-electron contributions and electronic Coulomb repulsion. See text for details. [c] X = O, N, F.

explicitly depend on the functional chosen. Any changes of these energy contributions are caused by the changes in geometry or the electron density itself. The functional-independent parts were therefore summed in a single contribution Σ. For hybrid functionals, the exchange energy is decomposed into the semilocal B88 and the exact HF contributions according to eq 3. The local exchange contribution is included in equal parts in the two components. The binding energy is then decomposed into the various terms as defined in eq 2 for the BLYP and in eqs 2 and 3 for the BHLYP functional.

Table 4 shows the contributions to the binding energy for the distonic ions **5a**, **6**, and **7** at equilibrium geometries calculated with the BLYP and the BHLYP functionals, respectively. For the weakly bound distonic ion **7** the components of the BLYP Kohn−Sham energy contribute equally to the binding energy. For the BHLYP functional the contribution of the exchange term is larger, but still low compared to common covalent bonding. These findings are both in line with the interpretation of distonic ion **7** as a loosely bound ion−dipole complex with no covalent bonding. The opposite situation is found for the strongly bound distonic ion **6**. The C−N bond is formed in large part due to a favorable exchange term (BLYP, 47.1 kcal/mol; BHLYP, 51.5 kcal/mol). Additionally, a significant contribution from correlation energy can be observed (BLYP, 9.0 kcal/mol; BHLYP, 11.9 kcal/mol), which must be expected for the formation of bonds with significant covalent character. The functional-independent part is slightly repulsive and reduces the binding energy for **6** by 4.1 kcal/mol and 5.1 kcal/mol for the BLYP and BHLYP functionals respectively.

For distonic ion **5a** the results for the BLYP functional are completely different from those obtained for the BHLYP functional. With the BLYP functional the major part of the binding energy arises from the functional-independent part, which amounts to 10.5 kcal/mol, whereas exchange contributes only 8.3 kcal/mol. Binding in distonic ion **5a** can therefore best be described as resulting from strong ion−dipole interactions, quite comparable to the situation in distonic ion **7**. With the BHLYP functional, on the other hand, the major contribution of 26.2 kcal/mol to the binding energy in distonic ion **5a** is due to the exchange term, 17.9 kcal/mol more than found at the BLYP level. The second remarkable point is the change of the functional-independent part $\Delta\Sigma$. For the BHLYP functional a repulsive contribution of −11.9 kcal/mol is found, compared with 10.5 kcal/mol attractive contribution for the BLYP functional. This pattern of energetic contributions is comparable to that found for distonic ion **6**. The covalent bonding in distonic ions **5a** and **6** described by the BHLYP functional corresponds to a repulsive functional independent term $\Delta\Sigma$, a large contribution from the exchange interaction ΔE_X, and a small amount of ΔE_C. The ion−dipole bonding in distonic ion **7** and **5a** described by the BLYP functional results from an attractive $\Delta\Sigma$, and a small contribution from the exchange and correlation terms ΔE_X and ΔE_C. These results are in line with the structural considerations mentioned above. Covalent bond formation results in a significant pyramidalization at C_1 and a short C−O bond length. Pure ion−dipole binding gives a planar ethylene radical moiety and a long C−O bond distance.

To gain some insight into the development of the contributing energy terms along the reaction pathway, calculations were performed at six selected values for the C−O bond in distonic ion **5a** (Table 4). All geometrical parameters except for the C−O bond length were optimized with the indicated functional and the 6-31+G(d,p) basis set. For each structure the binding energy was decomposed according to eq 2. The choice of the functional, i.e. BLYP vs BHLYP, has practically no influence on the distance dependence of the correlation energy, as the difference between correlation energy contributions never exceeds 0.2 kcal/mol. In contrast, comparison of the exchange energy contribution to the binding energy at a given distance is systematically larger by 3−6 kcal/mol at the BLYP level of theory as compared to the BHLYP level. This attractive contribution is overcompensated at the 1.6 Å geometry by the functional-independent energy $\Delta\Sigma$, which decreases by 7.9 kcal/mol compared to the BHLYP functional. The finding that the BLYP exchange contribution is more stabilizing at a fixed C−O bond distance of 16 Å is unexpected, as comparison of the components of the binding energy for distonic ion **5a** at the *equilibrium geometries* for each functional shows that for the BLYP functional the exchange contribution is of minor importance! A similar situation is also found for a fixed C−O bond distance of 2.1 Å. Again the BLYP exchange component is found to be more stabilizing by 3.3 kcal/mol compared to BHLYP. In contrast to the 1.6 Å geometry, the $\Delta\Sigma$ contribution for the BLYP and BHLYP functionals differs by only 0.5 kcal/mol now. The results for $\Delta\Sigma$ are depicted in Figure 2b.

The density functionals that we investigated belong to two different classes, the semilocal functionals such as BLYP and the nonlocal functionals that contain HF exchange such as BHLYP. We therefore additionally investigated the splitting of the total exchange into the semilocal and the HF contributions according to eq 3 in Table 4. Note that half of the local exchange contribution is contained in the semilocal $^1/_2\Delta E_{XB88}$ and half in the nonlocal $^1/_2\Delta E_{XHF}$, and that ΔE_X for BLYP contains both the local and semilocal contributions. The most remarkable point is the qualitative difference in the distance dependence of the DFT and the HF exchange part in the BHLYP

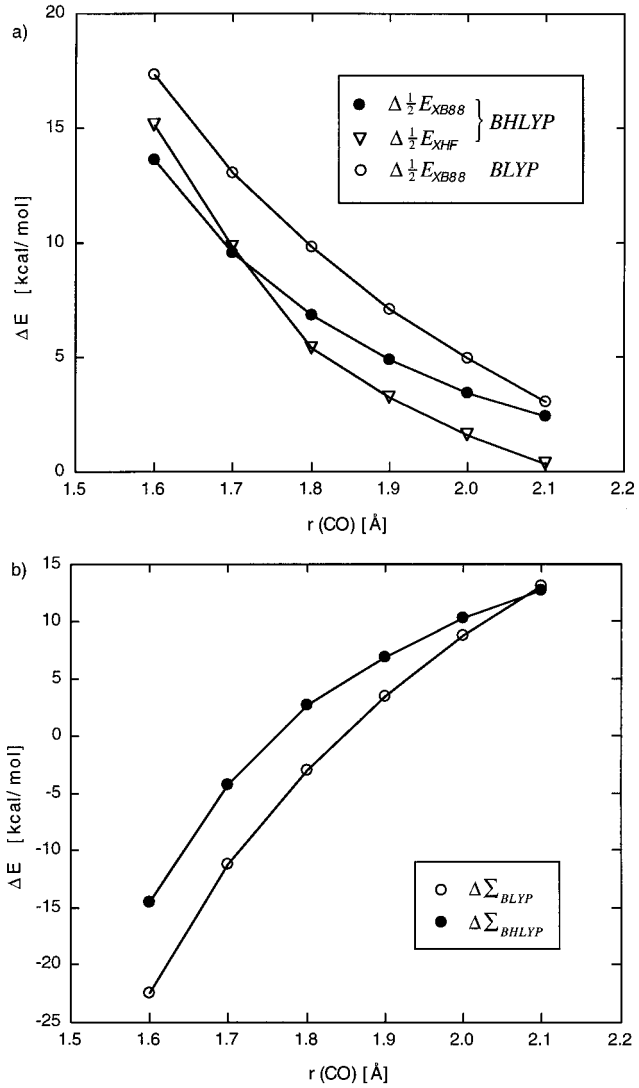

Figure 2. Distance dependence of components of the Kohn−Sham binding energy in distonic ion **5a**. Comparison of (a) the HF exchange and DFT exchange of BHLYP calculation with the B88 contribution of the BLYP calculation, and (b) the sum of the functional-independent terms.

functional. At large C−O distance the HF exchange part almost completely decays to zero, whereas the DFT exchange part contributes significantly to the binding energy. On the other hand, at short C−O bond distances the HF exchange part is even more stabilizing than the DFT exchange part of the BHLYP functional. Figure 2a depicts the BHLYP exchange energies $^1/_2\Delta E_{XB88}$ and $^1/_2\Delta E_{XHF}$ along the reaction pathway for the addition of water to ethylene radical cation. For better comparability with the BHLYP results the BLYP ΔE_X values were multiplied by a factor of 0.5. The general trend found for the BLYP functional is comparable to the DFT part of the BHLYP functional. A significant contribution of 2−3 kcal/mol to the binding energy is found for large bonding distance. To visualize the difference between the BLYP and BHLYP densities, we calculated single-point electron densities at the QCISD/6-311++G(2df,p) geometry. Figure 3 depicts the difference ρ(BHLYP) − ρ(BLYP) in the C_s-plane of **5a** generated by a modified version of the PROAIM package.[25] The first important observation is the negative areas in the immediate proximity of the nuclei. This shows that BLYP tends to localize the electron density closer to the nuclear positions than BHLYP. The innermost contour lines in these areas correspond to a charge density difference of $4 \times 10^{-2}e$.

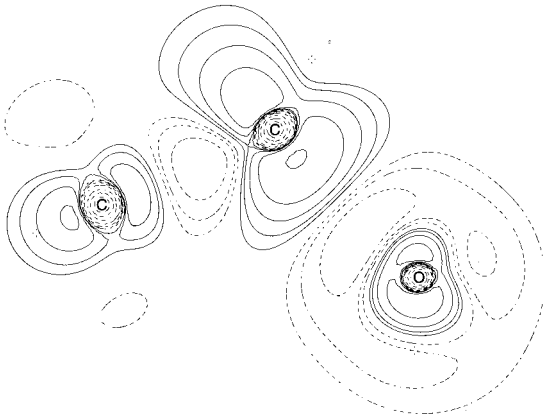

Figure 3. Difference between the BHLYP and BLYP total electron density of the distonic ion **5a** at the QCISD/6-311++G(2df,p) optimized geometry. The contour plane is the C_s mirror plane of **5a**. Solid lines represent positive and dashed lines represent negative values.

Secondly, a dumbbell-shaped positive area of higher BHLYP density at C_1 is found, whereas the extensive region around the oxygen atom is charge depleted. Assuming that C−O bond formation is accompanied by partial charge transfer from the nucleophile to the ethylene radical cation, this finding is in line with preferred bond formation in **5a** at the BHLYP level of theory.

Clusters. The goal of the present study is to investigate whether DFT is suitable to describe ethylene radical cation with bulk assemblies of water molecules. After the surprisingly disconcerting performance of BLYP for the monowater adduct **5a** we added water molecules successively to structure **5a** and determined equilibrium structures at the BLYP/6-31+G(d,p), BHLYP/631+G(d,p), and MP2/6-31+G(d,p) levels of theory. Table 3 summarizes the energetic and structural data found for these systems. Reaction of the hydrogen-bridged water dimer with ethylene radical cation gives adduct **5b** (Figure 1). The binding energy for the dissociation of structure **5b** into **1** and **2b** amounts to 42.9 kcal/mol for the BLYP functional. At the same time the *difference* of the C−O bond lengths between the methods is significantly reduced, compared to **5a**. For the BLYP functional a C−O distance of 1.657 Å is found, whereas MP2 yields 1.541 Å. For the adduct **5c**, derived from the water trimer and ethylene radical cation, this trend is continued. The binding energy for the dissociation of **5c** into **1** and **2c** is larger by another 20 kcal/mol and amounts to 61.7 kcal/mol. The difference in bond lengths is now reduced to 0.07 Å (BLYP, 1.584 Å; MP2, 1.513 Å). Thus, the more water molecules are added to the ethylene radical cation, the more reliable the BLYP calculations become. This shows that the problems of semilocal DFT methods with structure **5a** do not arise from the electronic situation itself, which is independent of the number of water molecules bound to ethylene radical cation, but appears to be a special problem with weak covalent bonding.

Conclusions

From our investigation of the distonic ions derived from the addition of hydrogen fluoride, water, and ammonia to ethylene radical cations employing density functional methods of different sophistication we must conclude that semilocal gradient-corrected DFT methods are not capable of describing the bonding in distonic ion **5a** $[C_2H_4{\cdot}H_2O]^{\bullet+}$. All these functionals, in particular BLYP, predict a strong ion−dipole interaction indicated by a long C−O bond distance, which contradicts other high-level ab initio results. For the distonic ions **6** $[C_2H_4{\cdot}H_3N]^{\bullet+}$ and **7** $[C_2H_4{\cdot}HF]^{\bullet+}$ the results are comparable at all investigated

levels of theory. Distonic ion **5a** $[C_2H_4{\cdot}H_2O]^{\bullet+}$ is special since it is located at the border between electrostatic and covalent binding. The BHLYP functional performs best of all employed density functionals in describing the binding in the distonic ions studied here and is consistent with the QCISD values. The analysis of the distance dependence shows that inclusion of HF exchange modifies the rate of decay of the exchange interaction with increasing distance of the reaction partners. Inclusion of HF exchange also induces a significant change of the electron density itself. Nevertheless, as shown by the examination of systems including two and three water molecules, BLYP performs ever better with an increasing number of water molecules. We therefore expect this method to be capable of describing the solution-phase chemistry of alkene radical cations.

Acknowledgment. This work was supported by the Volkswagen Stiftung and by Prof. H. Schwarz (TU-Berlin). Computational resources were provided by the Zuse-Rechenzentrum Berlin and the Zentraleinrichtung Rechenzentrum TU-Berlin. We appreciate the help of Dr. M. Frisch with the modification of the Gaussian94 code and the general support of Dr. J. Hutter with the CPMD code.

Note Added in Proof: Since the submission of this paper, Radom et al. have published new high-level theoretical data on the structure of distonic radical cation **5a**: Gauld, J. W.; Radom, L. *Chem. Phys. Lett.* **1997**, *275*, 28.

References and Notes

(1) (a) Caldwell, J.; Dang, L. X.; Kollman, P. *A. J. Am. Chem. Soc.* **1990**, 112, 9144. (b) Jorgensen, W. L.; McDonald, N. A.; Selmi, M.; Rablen, P. R. *J. Am. Chem. Soc.* **1995,** *117*, 11809.

(2) (a) Golding, B. T.; Radom, L. *J. Am. Chem. Soc.* **1976**, *98*, 6331. (b) Bouma, W. J.; Nobes, R. H.; Radom, L. *J. Am. Chem. Soc.* **1983**, *105*, 1743. (c) Yates, B. F.; Bouma, W. J.; Radom, L. *J. Am. Chem. Soc.* **1984**, *106*, 5805. (d) Postma, R.; Ruttink, P. J. A.; Van Baar, B.; Terlouw, J. K.; Holmes, J. L.; Burgers, P. C. *Chem. Phys. Lett.* **1986**, *123*, 409. (e) Gauld, J. W.; Radom, L. *J. Chem. Phys.* **1994**, *98*, 777.

(3) Zipse, H. *J. Am. Chem. Soc.* **1995**, *117*, 11798.

(4) Laasonen, K.; Sprik, M.; Parrinello, M. *J. Chem. Phys.* **1993**, *99*, 9080.

(5) (a) Marx, D.; Hutter, J.; Parrinello, M. *Chem. Phys. Lett.* **1995**, *241*, 457. (b) Marx, D.; Sprik, M.; Parrinello, M. *Chem. Phys. Lett.* **1997**, *272*, 360.

(6) (a) Tuckerman, M. E.; Laasonen, K.; Sprik, M.; Parrinello, M. *J. Phys.: Condens. Matter* **1994**, *6*, A93. (b) Tuckerman, M. E.; Laasonen, K.; Sprik, M.; Parrinello, M. *J. Phys. Chem.* **1995**, *103*,*150*.

(7) Car, R.; Parrinello, M. *Phys. Rev. Lett.* **1985**, *55*, 2471.

(8) Tschinke, V.; Ziegler, T. *Theor. Chim. Acta* **1991**, *81*, 65.

(9) (a) Becke, A. D. *Phys. Rev. A* **1988**, *38*, 3098. (b) Lee, C.; Yang, W.; Parr, R. G. *Phys. Rev. B* **1988**, *37*, 785.

(10) Hertwig, R.; Koch, W. *J. Comput. Chem.* **1995**, *16*, 576.

(11) Ventura, O. N.; Kieninger, M. *Chem. Phys. Lett.* **1995**, *245*, 488.

(12) Becke, A. D. *J. Chem. Phys.* **1993**, *98*, 1372.

(13) *Gaussian 94* (Revision B.3); Frisch, M., Trucks, G. W., Schlegel, H. B., Gill, P. M. W., Johnson, G., Robb, M. A., Cheeseman, J. R., Keith, T. A., Peterson, G. A., Montgomery, J. A., Raghavachari, K., Al-Laham, M. A., Zakrzewski, V. G., Ortiz, J. V., Foresman, J. B., Cioslowski, J., Stefanov, B. B., Nanayakkara, A., Challacombe, M., Peng, C. Y., Ayala, P. Y., Chen, W., Wong, M. W., Andres, J. L., Replogle, E. S., Gomperts, R., Martin, R. L., Fox, D. J., Binkley, J. S., Defrees, D. J., Baker, J., Stewart, J. P., Head-Gordon, M., Gonzales, C., Pople, A. J. Gaussian Inc.: Pittsburgh, PA, 1995.

(14) Laming, G. J.; Handy, N. C.; Amos, R. D. *Mol. Phys.* **1993**, *80*, 1121.

(15) Baker, J.; Scheiner, J.; Andzelm, A. J. *Chem. Phys. Lett.* **1993**, *216*, 380.

(16) Hutter, J.; Ballone, P.; Bernasconi, M.; Focher, P.; Fois, E.; Goedecker, S.; Parrinello, M.; Tuckerman, M. *CPMD Version 3.0*; MPI fur Festkorperforschung and IBM Research: 1990-96.

(17) Troullier, N.; Martins, J. L. *Phys. Rev. B* **1991**, *43*, 1993.

(18) Stephens, W.; Basch, H.; Krauss, J. *J. Chem. Phys.* **1984**, *81*, 6026.

(19) Köppel, H.; Cederbaum, L. S.; Domcke, W.; Shaik, S. S. *Angew. Chem.* **1983**, *95*, 221.

(20) Merer, A. J.; Schoonveld, L. *J. Chem. Phys.* **1968**, *48*, 522.

(21) Köppel, H.; Domcke, W.; Cederbaum, L. S.; von Niessen, W. *J. Chem. Phys.* **1978**, *69*, 4252.

(22) Buenker, R. J.; Peyerimhoff, S. D.; Hsu, L. H. *Chem. Phys. Lett.* **1971**, *11*, 65.

(23) Vosko, S. H.; Wilk, L.; Nusair, M. *Can. J. Phys.* **1980**, *58*, 1200.

(24) Perdew, J. P. *Phys. Rev. B* **1986**, *33*, 8822.

(25) Biegler-Konig, F. W.; Bader, R. F. W.; Tang, T. *J. Comput. Chem.* **1982**, *3*, 317.